Arch. Metall. Mater. **68** (2023), 1, 155-159

DOI: https://doi.org/10.24425/amm.2023.141489

SEONG-MIN SO[1], KI-YEON KIM[1], IL-SONG PARK[1], SEOK-JAE LEE[1],
DONG-JIN YOO[2], YEON-WON KIM[3*], MIN-SUK OH[1*]

IMPROVEMENT OF WELDABILITY OF HOT-DIP GALVANIZED STEEL BY ANTI-GALVANIZING COATING WITH Si-Fe-Al OXIDE-BASED MICROPOWDER

A Si-Fe-Al ternary oxide-based micropowder coating was used to prevent the formation of a Zn coating on steel during the hot-dip Zn galvanizing process to reduce the welding fume and defects generated during the welding of Zn-galvanized steel. The composition ratio of the oxide powder was optimized and its microstructure and weldability were evaluated. The optimized oxide coating was stable in the hot-dip galvanizing bath at 470°C and effectively inhibited the formation of Zn coating. The Zn residue could be easily removed with simple mechanical impact. The proposed coating reduced Zn fume and prevented the residual Zn from melting in the weld bead during high-temperature welding, thus reducing the number of welding defects. The results indicated that this pretreatment can simplify the manufacturing process and shorten the process time cost-effectively.

Keywords: Hot-dip galvanizing; Anti-galvanizing; Oxide micropowder; Weldability

1. Introduction

Hot-dip galvanizing is a surface treatment method that improves the corrosion resistance of steel through the sacrificial protection of Zn and the barrier effect of the corrosion product formed on the surface [1,2]. It is widely used in various industrial applications such as automobiles, shipbuilding, and construction [3-5]. High-temperature fusion-based welding is one of the most important technologies for metal-to-metal bonding in the production of steel-based products [6,7]. However, when Zn galvanized steel is welded, Zn, a metal with a low melting temperature, tends to evaporate due to high welding heat. In this process, the Zn fume that does not escape from the molten metal causes welding defects such as blowholes, pits, and spatters [8-10]. In addition, because Zn fume causes respiratory diseases that deteriorate the health of workers, very careful management is required in the workplace [11-13]. Therefore, to prevent the generation of Zn fume and the consequent occurrence of health risks and welding defects, the Zn coating layer must be removed in the welding area for Zn galvanized products such as iron columns, shell plates, and ballasts [8,14]. Masking methods such as duct taping or shop primer painting are widely used to prevent the formation of Zn coating in specific areas. However, high pot temperatures above 450°C thermally damage the tape chemicals, resulting in the formation of an unwanted Zn coating, which is removed by employing additional operations such as grinding before welding.

Because these additional processes increase the costs and reduce the efficiency of masking methods, various studies have been conducted to develop efficient anti-galvanizing (AG) methods for reducing welding defects and production costs. Anti-coating agents with a polycarbonate-based compound binder and release agents such as polytetrafluoroethylene (PTFE) and MoS_2-based compounds have been shown to induce easy delamination of the Zn coating layer owing to the difference in the thermal expansion of the constituents [15,16]. Calcium carbonate and ultrafine colloidal silica sol coatings can prevent molten Zn from adhering to the steel surface [17,18]. Mechanical installation of jig units and devices has also been introduced to prevent the formation of Zn coating [19]. However, these AG methods require the use of expensive materials and additional mechanical devices, and hence provide low manufacturing productivity. In addition, an easy method for removing Zn residues from the surface after the galvanizing process is yet to be developed.

[1] JEONBUK NATIONAL UNIVERSITY, DIVISION OF ADVANCED MATERIALS ENGINEERING, JEONJU, REPUBLIC OF KOREA
[2] JEONBUK NATIONAL UNIVERSITY, DEPARTMENT OF ENERGY STORAGE/CONVERSION ENGINEERING OF GRADUATE SCHOOL, DEPARTMENT OF LIFE SCIENCE, HYDROGEN AND FUEL CELL RESEARCH CENTER, JEONJU, REPUBLIC OF KOREA
[3] MOKPO NATIONAL MARITIME UNIVERSITY, DIVISION OF MARINE MECHATRONICS, MOKPO, REPUBLIC OF KOREA

* Corresponding authors: misoh@jbnu.ac.kr, k.yeonwon@mmu.ac.kr

In this study, we introduce a new AG technology using a micropowder coating based on Si, Fe, and Al ternary oxides. The coating could be easily applied, was stable in the hot-dip galvanizing bath above 450°C, and could be easily removed after galvanizing. The composition ratio of the powder was optimized and its microstructure and weldability were evaluated.

2. Experimental

SiO_2 (Shinyo Pure Chemicals Co., Ltd.), Fe_2O_3 (Junsei Chemical Co., Ltd.), and Al_2O_3 (Daejung Chemicals & Metals Co., Ltd.) (SFA) micropowders were mixed with water and stirred to prepare an SFA solution. A 0.8 mm-thick commercial quality (CQ) steel sheet (POSCO Co., Ltd.) was cut into 30 mm × 150 mm strips and used as the substrate. Before SFA coating, to remove the impurities and oxides remaining on the surface, the steel was degreased by immersing in a 10% NaOH solution at 60°C for 10 min, followed by pickling in 10% HCl for 10 min and rinsing in water. Then, a flux layer was formed by immersing in a $ZnCl_2 \cdot 3NH_4Cl$ mixed solution at 60°C to enhance the diffusion reaction between molten Zn and the Fe substrate. The substrate was then immersed in the SFA solution and dried in an oven at 120°C for 5 min. TABLE 1 lists the weight ratio of each of the SFA solution tested. For comparison, duct-taped and shop primer-painted samples were also prepared. Hot-dip galvanizing was carried out after drying the prepared samples at 120°C to prevent the explosion due to the expansion of moisture. The temperature of the Zn pot was 470°C, and the immersion time was 5 min. After the solidification of the Zn coating, the samples were immobilized and impacted 20 times using a reciprocating impact device with a force of 3 N to remove the coating residue.

TABLE 1

Weight ratios of the SiO_2, Fe_2O_3 and Al_2O_3 powder mixed solutions

Sample	Composition (wt.%)			
	SiO_2	Al_2O_3	Fe_2O_3	Water
SA	25	25	0	50
SFA10	20	20	10	50
SFA20	15	15	20	50
SFA30	10	10	30	50

To evaluate the weldability of the steel, single lap joints were fabricated by gas metal arc welding (GMAW) using the galvanized steel produced using each AG method. Ar (flow rate = 20 L/min) was used as the protective gas. The welding current, voltage, and speed were 150 A, 20 V, and 150 mm/min, respectively. The amount of Zn fume was visually compared, and the welding defects were investigated by analyzing the cross-sectional microstructure of the welding bead using optical microscopy (OM) (DM2500, Leica) and field-emission scanning electron microscopy (FE-SEM) (SU-70, HITACHI). The chemical composition of the coating layer was determined using energy-dispersive X-ray spectroscopy (EDS). Depth profiling was carried out using a glow discharge spectroscopy (GDS) (JY 10000 RF, Jobin Yvon) using a voltage of 700 V and a constant current of 20 mA under an Ar pressure of 10 MPa. The analyzed area had a diameter of approximately 4 mm.

3. Results and discussion

Fig. 1 shows the OM and FE-SEM images showing the coatability and microstructure of the oxide-based powder coating layers with (SFA20; 25% each SiO_2 and Al_2O_3 (SA) and 15% each SiO_2 and Al_2O_3 with 20% Fe_2O_3) and without Fe_2O_3. In the case of SA without Fe_2O_3, the substrate was not fully covered and the Fe-exposed area was large. The FE-SEM image in Fig. 1(c) shows that pores and voids were largely formed between the SiO_2 and Al_2O_3 powders. The poor coatability of SA can be attributable to this empty space between the powders, which caused the SA powder to fall off the surface during the drying process. In contrast, when Fe_2O_3 nanopowder was added, the Fe-exposed area decreased remarkably and a uniform composite coating layer was formed on the surface, as shown in Fig. 1(b). The image analysis showed that the Fe exposure areas of the SA, SFA10, SFA20, and SFA30 samples were 31.2, 15.6, 0.9, and 0.1%, respectively. From Fig. 1(d), it can be observed that the Fe_2O_3 nanopowder densely infiltrated the space between the SiO_2 and Al_2O_3 micropowders, increasing the bonding strength between them. The increase in the bonding strength of the elements with increasing Fe_2O_3 content was due to the magnetic properties of Fe_2O_3. This is consistent with the results reported previously for porous $Na_2Ti_6O_{13}$ thin films[20]. In addition, the increase in the viscosity of the water-based Fe_2O_3 nanofluid partially affected the decrease in the porosity of the coatings [21].

Fig. 2 shows the samples before and after hot-dip galvanizing with and without the AG pre-treatment using duct tape, shop primer paint, and SFA20. After hot-dip galvanizing, the sample without the AG coating showed a uniform and defect-free Zn coating. In contrast, in the AG-treated samples, the Fe substrate was covered with messy, roughly stuck Zn that did not alloy with the substrate because of the suppressed interfacial alloying reaction between the substrate and molten Zn due to the AG layer. To evaluate the ease of removal of the Zn roughly stuck on the AG-covered area, repeated mechanical impact was applied to the area. Image analysis showed that about 25% of the Zn remained on the surface of the samples with duct tape and primer painting. On the other hand, Zn was completely removed by simple mechanical impact in the case of the SFA20 sample. This can be attributed to the decrease in the wettability of molten Zn by SiO_2, Fe_2O_3, and Al_2O_3, hindering the inter-diffusion reaction between molten Zn and the substrate.

To further investigate the chemical residues on the Zn-removed area, the areas marked with circles in Fig. 2 were examined using FE-SEM and GDS (Fig. 3). Heat-damaged chemical substances were observed on the surface of the duct-taped sample, as shown in Fig. 3(a). EDS measurements revealed that they were the chemical components of the duct tape such as

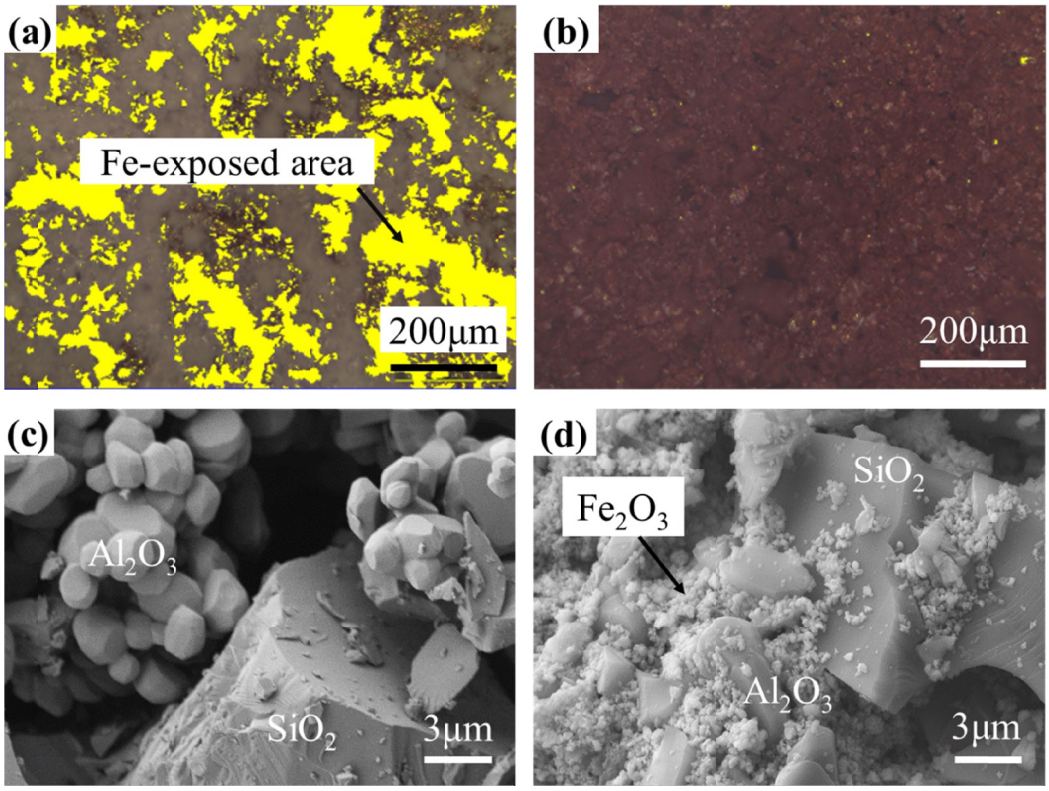

Fig. 1. Microstructures of the SFA coating layers with different oxide powder compositions: (a) OM and (c) FE-SEM images of the SA-treated steel sample, and (b) OM and (d) FE-SEM images of the SFA20-treated steel sample

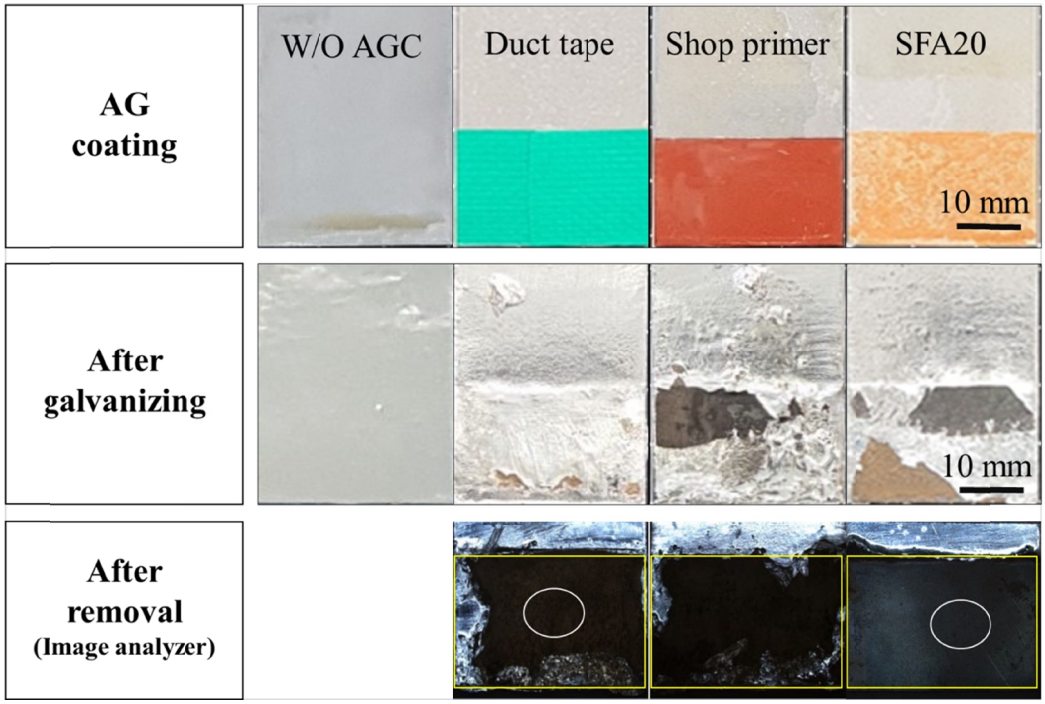

Fig. 2. Samples before and after hot-dip galvanizing with and without the AG pre-treatment using duct tape, shop primer paint, and SFA20

5.1-13.3 wt% C, 1.4-1.5 wt% Ca and 17.7-32.4 wt% O. The GDS depth profile (Fig. 3(c)) indicated that the thickness of the chemical residue was approximately 2-3 μm. These results indicate that the duct-taped sample required an additional removal process such as grinding. On the other hand, in the case of SFA20, only trace amounts of Al and Si remained, and the thickness of the residue less than 0.2 μm.

To evaluate the weldability of the samples, single lap joints were fabricated by GMAW using the galvanized steel produced with each AG method as shown schematically in Fig. 4(a). Visual

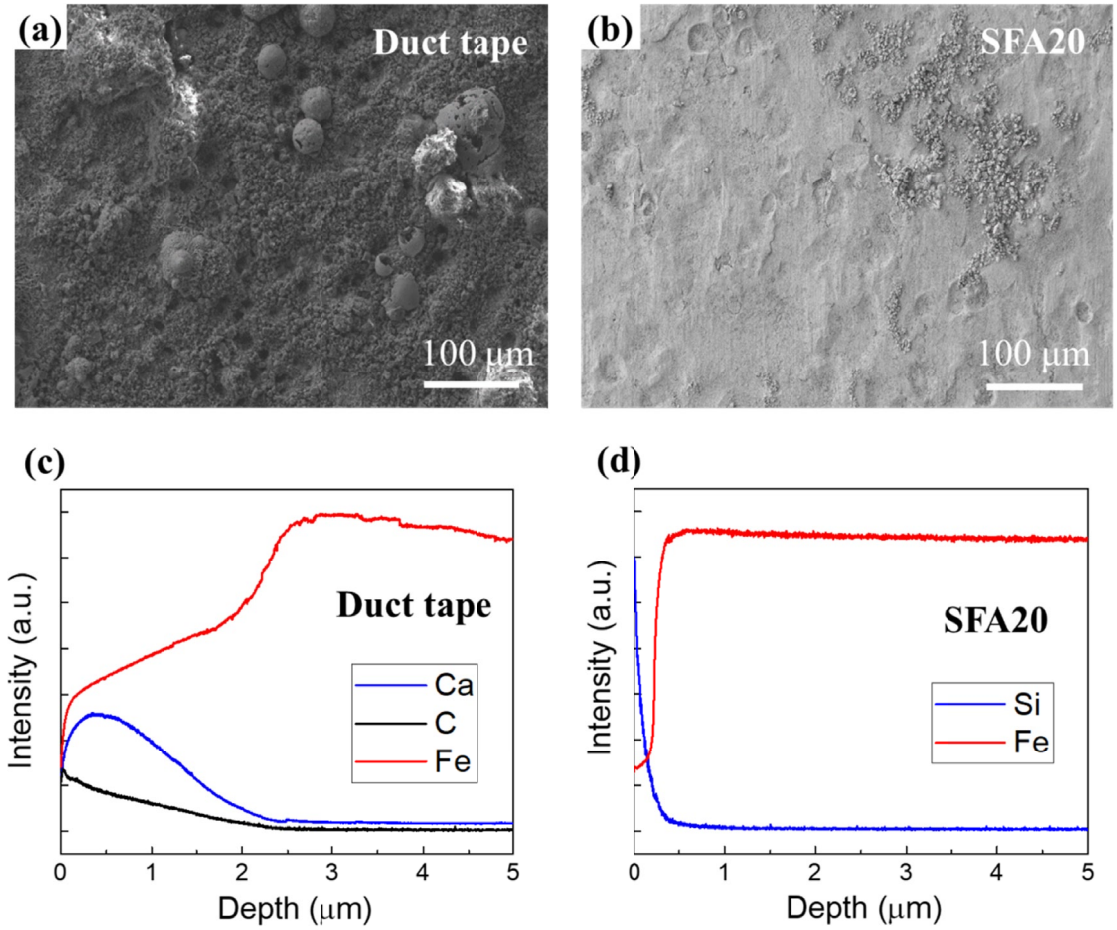

Fig. 3. (a), (b) FE-SEM images and (c), (d) GDS depth profiles of the surfaces marked with circles in Fig. 2 after removing the Zn residue

inspection revealed the SFA20 sample produced significantly reduced Zn fumes during the welding process as compared to the duct-taped sample because of the effective removal of Zn residue. The microstructure of the weld bead marked with a rectangle in Fig. 4(a) was observed to analyze the welding defects. The FE-SEM results revealed that an Fe-Zn intermediate phase was formed inside the weld bead of the duct-taped sample. This weld bead consisted of approximately 3-5 wt% Zn, as indicated by the EDS results. This can be attributed to the reaction of Fe with molten Zn (melted during high-temperature welding). In addition, a large number of gas holes and small cavities were observed in the duct-taped sample, as shown in Fig. 4(c), which were formed by the vaporization of the residual Zn and/or tape chemicals by heat during high-temperature welding. These holes and cavities were discharged in the form of gas [22]. It has been reported that during the welding of galvanized steel, the vaporization of Zn not only forms gas holes, but also destabilizes the arc, causing the generation of defects such as spatters, which leads to the deterioration of the mechanical properties of the weld [22,23]. In contrast, in the case of SFA20, because the roughly stuck Zn layer was completely removed, welding defects such as the Fe-Zn intermediate phase and gas holes were not observed, as shown in Fig. 4(d). This indicates that the SFA coating could prevent the residual Zn from melting in the weld bead during high-temperature welding.

4. Conclusions

In this study, an AG pretreatment using SiO_2, Fe_2O_3, and Al_2O_3 powders was employed to reduce the welding fume and defects that occur during the welding of Zn galvanized steel. The Fe_2O_3 nanopowder infiltrated and filled the empty space between the SiO_2 and Al_2O_3 powders, increasing the bonding strength of the powder, which led to the formation of a uniform and barespot-free coating layer. With optimized SFA coating, Zn was easily removed by simple mechanical impact due to the lowered wettability of molten Zn by SiO_2, Fe_2O_3, and Al_2O_3 oxide. The SFA coating effectively prevented the residual Zn from melting in the weld bead during high-temperature welding, thus reducing the number of welding defects such as the Fe–Zn intermediate phase and gas holes.

Acknowledgements

This work was supported by the [National Research Foundation of Korea (NRF)] grant funded by the Korea Government (Ministry of Science and ICT) [No. 2022R1A2C1008972]. This work was also supported by the Technology Innovation Program (20012941, 20016850) funded by the Ministry of Trade, Industry & Energy (MOTIE, Korea). This work was also supported in part by “Research Base Construction Fund Support Program”

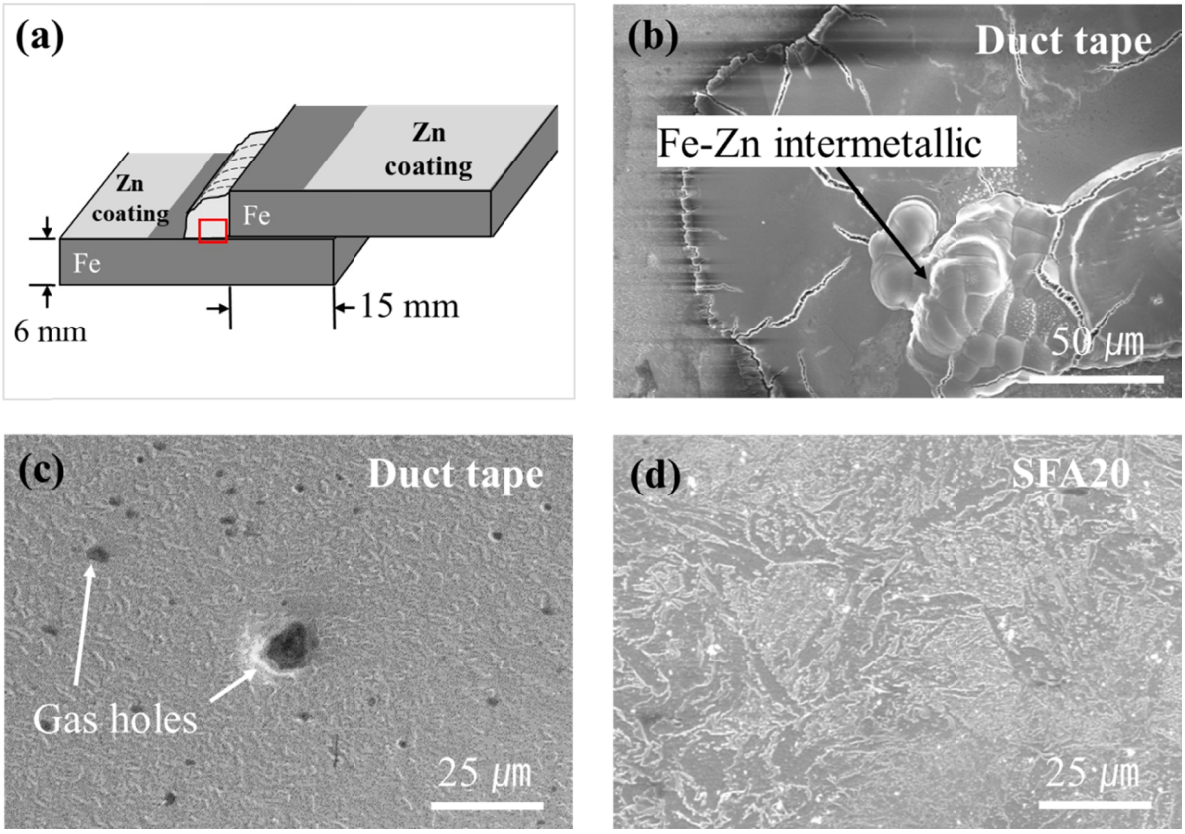

Fig. 4. (a) Schematic diagram of the single lap joints and microstructures of the weld bead for (b), (c) duct tape and (d) SFA20

funded by Jeonbuk National University in 2021. This work was also supported by a Korea Institute for Advancement of Technology grant, funded by the Korea Government (MOTIE) (P0002019), as part of the Competency Development Program for Industry Specialists.

REFERENCES

[1] C. Soriano, A. Alfantazi, Constr. Build. Mater. **102**, 904-912 (2016).
[2] M.S. Oh, S.H. Kim, J.S. Kim, J.W. Lee, J.H. Shon, Y.S. Jin, Met Mater. Int. 22, 26-33 (2016).
[3] C. Qiao, L. Shen, L. Hao, X. Mu, J. Dong, W. Ke, J. Liu, B. Liu, J. Mater. Sci. Technol. **35**, 2345-2356 (2019).
[4] S.M. Joo, Y.G. Kim, Y.J. Kwak, D.J. Yoo, C.U. Jeong, J.P. Park, M.S. Oh, Materials, **14**, 6756 (2021).
[5] L. Chen, R. Fourmentin, J.R. McDermid, Metall. Mater. Trans. A **39A**, 2128-2142 (2008).
[6] P. Andreazza, A. Gericke, K.M. Henkel, Weld. World **65**, 1199-1210 (2021).
[7] M. Uchihara, Weld. Int. **25**, 249-259 (2011).
[8] Y.M. Lim, B.S. Jang, J.H. Koh, J. Weld. Join. **30**, 440-444 (2012).
[9] S.M. Shin, S.H. Rhee, Metals **8**, 1077 (2018).
[10] J. Ma, F. Kong, B. Carlson, R. Kovacevic, Mitigating zinc vapor induced weld defects in laser welding of galvanized high-strength steel by using different supplementary means, Intech Open Access Publisher (2012).
[11] L. Hartmann, M. Bauer, J. Bertram, M. Gube, K. Lenz, U. Reisgen, T. Schettgen, T. Kraus, P. Brand, Int. J. Hyg. Envir. Heal. **217**, 160-168 (2014).
[12] J. Bleidorn, H.A. Krabbe, B. Gerhards, T. Kraus, P. Brand, J. Krabbe, C. Martin, Sci. Rep. **9**, 1-10 (2019).
[13] J. Krabbe, V. Beilmann, B. Gerhards, A. Markert, K. Thomas, T. Kraus, P. Brand, J. Occup. Environ. Med. **61**, 8-15 (2019).
[14] https://galvanizeit.org/design-and-fabrication/fabrication-considerations/welding/welding-galvanized-steel
[15] D.H. Lee, D.Y. Seo, A partial inhibitor of hot dip galvanizing and method of hot dip galvanizing using the same, Patent KR 102082963 B1 (2020).
[16] D.H. Lee, D.Y. Seo, C.S. Kim, Manufacturing method for a partial inhibitor of hot dip galvanizing, Patent KR 101988631 B1 (2019).
[17] E. Moroni, Selective galvanizing process using a calcium carbonate masking composition, Patent US 04421793 A (1983).
[18] N.M. Adams, Silica sol-masking in galvanizing process, Patent US 03117085 A1 (1965).
[19] S.J. Choi, S.K. Kim, Selective plating device, Patent KR 1020160057734 A (2016).
[20] K.S. Yun, H.K. Ku, W.S. Kang, S.J. Kim, Corros. Sci. Technol. **11**, 65-69 (2012).
[21] L. Colla, L. Fedele, M. Scattolini, S. Bobbo, Adv. Mech. Eng. **2012**, 1-8 (2012).
[22] G. Ma, H. Yuan, L. Yu, Y. He, Mater. Manuf. Process **36**, 1178-1188 (2021).
[23] Z. Mu, X. Chen, R. Hu, S. Lin, S. Pang, J. Phys. D Appl. Phys. **53**, 075202 (2020).